Evaluation of stratospheric age of air from CF_4, C_2F_6, C_3F_8, CHF_3, HFC-125, HFC-227ea and SF_6; implications for the calculations of halocarbon lifetimes, fractional release factors and ozone depletion potentials

Emma Leedham Elvidge[1], **Harald Bönisch**[2], **Carl A. M. Brenninkmeijer**[3], **Andreas Engel**[4], **Paul J. Fraser**[5],
Eileen Gallacher[1], **Ray Langenfelds**[5], **Jens Mühle**[6], **David E. Oram**[1], **Eric A. Ray**[7,8], **Anna R. Ridley**[1],
Thomas Röckmann[9], **William T. Sturges**[1], **Ray F. Weiss**[6], and **Johannes C. Laube**[1]

[1]School of Environmental Sciences, University of East Anglia, Norwich Research Park, Norwich, NR4 7TJ, UK
[2]Institute of Meteorology and Climate Research, Karlsruhe Institute of Technology, Karlsruhe, Germany
[3]Atmospheric Chemistry Division, Max Planck Institute for Chemistry, Mainz, Germany
[4]Institute for Atmospheric and Environmental Sciences, Goethe University of Frankfurt, Frankfurt, Germany
[5]Climate Science Centre, CSIRO Oceans and Atmosphere, Aspendale, Victoria, Australia
[6]Scripps Institution of Oceanography, University of California, San Diego, La Jolla, California, USA
[7]Chemical Sciences Division, Earth Systems Research Laboratory, NOAA, Boulder, Colorado, USA
[8]Cooperative Institute for Research in Environmental Sciences, University of Colorado, Boulder, Colorado, USA
[9]Institute for Marine and Atmospheric Research Utrecht, Utrecht University, Utrecht, the Netherlands

Correspondence: Emma Leedham Elvidge (e.leedham-elvidge@uea.ac.uk)

Abstract. In a changing climate, potential stratospheric circulation changes require long-term monitoring. Stratospheric trace gas measurements are often used as a proxy for stratospheric circulation changes via the "mean age of air" values derived from them. In this study, we investigated five potential age of air tracers – the perfluorocarbons CF_4, C_2F_6 and C_3F_8 and the hydrofluorocarbons CHF_3 (HFC-23) and HFC-125 – and compare them to the traditional tracer SF_6 and a (relatively) shorter-lived species, HFC-227ea. A detailed uncertainty analysis was performed on mean ages derived from these "new" tracers to allow us to confidently compare their efficacy as age tracers to the existing tracer, SF_6. Our results showed that uncertainties associated with the mean age derived from these new age tracers are similar to those derived from SF_6, suggesting that these alternative compounds are suitable in this respect for use as age tracers. Independent verification of the suitability of these age tracers is provided by a comparison between samples analysed at the University of East Anglia and the Scripps Institution of Oceanography. All five tracers give younger mean ages than SF_6, a discrep-
ancy that increases with increasing mean age. Our findings qualitatively support recent work that suggests that the stratospheric lifetime of SF_6 is significantly less than the previous estimate of 3200 years. The impact of these younger mean ages on three policy-relevant parameters – stratospheric lifetimes, fractional release factors (FRFs) and ozone depletion potentials – is investigated in combination with a recently improved methodology to calculate FRFs. Updates to previous estimations for these parameters are provided.

1 Introduction

The "mean age of air" (mean AoA), defined as the average time that an air parcel has spent in the stratosphere, is an important derived quantity used in several stratospheric research fields, often when direct physical or chemical measurements are scarce, not available or inadequate. AoA is perhaps best known for being a measure of the strength of

the Brewer–Dobson circulation (BDC) and as a means of determining air mass fluxes between the troposphere and stratosphere (Bönisch et al., 2009). It is also used in calculations to determine the state of recovery of the ozone layer via its role in calculations of stratospheric lifetimes, ozone depletion potentials (ODPs; Brown et al., 2013; Laube et al., 2013; Volk et al., 1997) and effective equivalent stratospheric chlorine (Newman et al., 2006).

Mean ages can be derived by comparing an observed abundance of a stratospheric tracer to the tropospheric time series of that gas, assuming that the trace gas in question is largely chemically inert in the stratosphere and has a monotonically, ideally linearly, changing tropospheric concentration (Hall and Plumb, 1994). Commonly used tracers include sulfur hexafluoride (SF_6) and carbon dioxide (CO_2), which have been used extensively to track large-scale stratospheric transport and transport trends and to evaluate atmospheric residence times of ozone-depleting substances (ODSs) and their impact on the ozone layer (Andrews et al., 2001; Engel et al., 2002; Volk et al., 1997). There are, however, problems with using these compounds as age tracers. The limitations of CO_2 have been recently outlined in detail by Engel et al. (2017) and include a complicated tropospheric trend – in part due to the influence of its seasonal cycle (Bönisch et al., 2009) – and a stratospheric CO_2 source, i.e. the oxidation of hydrocarbons. For SF_6, recent research suggests its lifetime has likely been overestimated, and thus it may be giving high-biased mean ages. The evidence for a proposed reduction in SF_6 lifetime comes from both modelling and measurement studies, which have evaluated its stratospheric loss mechanisms via electron attachment (most recently by Kovács et al., 2017) and in the polar vortex (Andrews et al., 2001; Ray et al., 2017). The most recent (at the time of writing) evaluation gives a revised lifetime of 850 (580–1400) years (Ray et al., 2017). This is considerably lower than the 3200-year lifetime used in the most recent assessments of the Intergovernmental Panel on Climate Change (IPCC, 2013) and the World Meteorological Organization (WMO, 2014). A revised lifetime will impact the estimated global warming potential of SF_6 (Kovács et al., 2017). These limitations do not preclude the use of CO_2 and SF_6 as age tracers, but may require complex corrections or limit the suitability of these gases to act as tracers in certain regions (Andrews et al., 2001; Bönisch et al., 2009). With this study, we do not attempt to discredit these extremely useful existing age tracers, but to add to the range of available tracers to improve the overall understanding in this field.

As mentioned above, AoA is an important component in our understanding of the BDC. The potential changes to the BDC as the troposphere warms are not yet fully understood. Chemistry–climate models predict an increase in the strength of the BDC (e.g. Li et al., 2008; Oberländer et al., 2013), which would be observed as a negative trend in (or a move to younger) mean ages. However, a time series of mean ages derived from stratospheric observations of trace gases in the mid-latitudes above 25 km has not found a significant trend over the past 40 years (Engel et al., 2009, 2017). Stratospheric circulation is complex: the shallow and deep branches of the BDC may be changing at different rates (Bönisch et al., 2011; Diallo et al., 2012; Ray et al., 2014) and shorter-timescale dynamical changes driven by the quasi-biennial oscillation or the El Niño–Southern Oscillation may complicate or even mask long-term changes to the BDC (Mahieu et al., 2014; Stiller et al., 2017). For this reason, if chemical tracers are to be used to diagnose global changes to the BDC they must be chemically inert throughout the stratosphere. Unfortunately, the influence of SF_6-depleted mesospheric air in the upper stratosphere (potential temperature > 800 K) and the higher Southern Hemisphere latitudes (poleward of 40° S) may bias SF_6-derived mean ages in these regions (Stiller et al., 2017).

The combination of the need for accurate age tracers to track stratospheric circulation changes and the uncertainties surrounding existing age tracers prompted us to investigate a suite of anthropogenic trace gases with stratospheric lifetimes > 100 years to identify other potential AoA tracers. Of particular interest are the alkane-derived perfluorocarbons (PFCs), which are extremely long-lived, stable trace gases (WMO, 2014), at least one of which, perfluoromethane (CF_4), was previously shown to have potential as an age tracer (Harnisch et al., 1999). In this paper, we assess the use of six alternative stratospheric age tracers[1]: CF_4, perfluoroethane (C_2F_6), perfluoropropane (C_3F_8), trifluoromethane (CHF_3), pentafluoroethane (HFC-125) and 1,1,1,2,3,3,3-heptafluoropropane (HFC-227ea) and compare them with the existing age tracer SF_6. An overview of all compounds discussed in this paper, including current stratospheric lifetime estimates and tropospheric growth rates, can be found in Table 1.

Supporting the potential use of "new" age tracers is the increasing number of methods available for collecting stratospheric air samples. Recently, air from the novel AirCore method has been used to calculate CO_2-derived mean ages (Engel et al., 2017) and lightweight stratospheric bag samplers have also been developed (Hooghiem et al., 2017). These technologies provide an excellent opportunity to increase the temporal and spatial coverage of stratospheric measurements in an affordable manner. However, it is important that the mean ages derived from these air samples (which may, in the case of discrete air samples, be as little as 20 mL of air per sample) have a similar level of uncertainty as more traditional samplers (i.e. large balloon-borne cryosamplers and high-altitude research aircraft; Sect. 2), especially if we wish to compare changes in mean ages over time. In

---

[1]To enhance the readability of this paper we have selected the most common name for each compound to use as its abbreviation, even if this means mixing chemical conventions (e.g. CHF_3 but HFC-227ea). Full details for each compound are provided in Table 1.

Table 1. Overview of trace gases used in this study and their relevant properties.

Compound	Formula	Stratospheric lifetime (yr) (WMO, 2014)	Growth rate %[a]	Average measurement precision %[b]	Number of samples in tropospheric time series
Perfluoromethane, PFC-14	CF_4	$> 50\,000$[c]	0.90	0.2	219
Perfluoroethane, PFC-116	C_2F_6	$> 10\,000$	2.8	1.6	114
Perfluoropropane, PFC-218	C_3F_8	~ 7000	7	1.9	34
Trifluoromethane, HFC-23	CHF_3	4420	4.2	1.7	117
Pentafluoroethane, HFC-125	C_2HF_5	351	17	1.1	40
Heptafluoropropane, HFC-227ea	C_3HF_7	673	14	2.8	29
Sulfur hexafluoride	SF_6	3200 (850[d])	4	1.1	59

[a] Growth rates are annual values averaged from 2002–2012 and derived from our own records, apart from CF_4, which is from the SIO AGAGE CG time series 2004–2017 (Sect. 2), and SF_6, for which higher-frequency 2004–2014 NOAA data are used (see Fig. S1 for agreement between NOAA and UEA data). [b] Precision calculations are outlined in Sect. 2. Here the precision is calculated only for the tropospheric time series data. Stratospheric sample precisions are in Table 2. [c] Total atmospheric lifetime. [d] Ray et al. (2017).

Sect. 3 we provide details of our uncertainty analysis to facilitate similar analyses on future mean age calculations.

We investigated this set of tracers for a variety of reasons. Firstly, we selected several tracers – CF_4, C_2F_6, C_3F_8 and CHF_3 – with estimated stratospheric lifetimes greater than SF_6 (Table 1) because of their potential to be suitably inert age tracers. Secondly, we selected a tracer – HFC-227ea – with a lifetime shorter than (the currently established) SF_6 lifetime to provide a contrasting point of comparison. Recently, the SF_6 lifetime has been shown to be perhaps closer to HFC-227ea than previously thought (Ray et al., 2017; Table 1) and so we include it in our comparison. Finally, we included HFC-125 as a potential age tracer as we believe its current estimated stratospheric lifetime of 351 years (SPARC, 2013; derived from model outputs) is potentially an underestimate based on preliminary mean age interpretations at UEA (finalised data included throughout this paper). We believe the lifetime of HFC-125 (C2, CHF_2CF_3) should fall between CHF_3 (C1) and HFC-227ea (C3, $CHF_2CF_2CF_3$). All seven of the above-mentioned tracers currently fulfil the prerequisite of having well-constrained monotonically increasing growth rates in the troposphere.

2 Methodology

Long-term tropospheric time series are required to define the input of each tracer to the stratosphere. No definition of "long-term" has been set, but several studies use a period of 10–15 years leading up to the stratospheric measurement period as a suitable tropospheric time series input for mean age calculations of 0–8 years or even up to 10 years if a time series at the later end of this range is used (Engel et al., 2002, 2006; Haenel et al., 2015). The University of East Anglia (UEA) has analysed whole air samples from the Cape Grim Baseline Air Pollution Station in Tasmania, Australia (https://agage.mit.edu/stations/cape-grim) since 1978 for all compounds discussed in this paper except CF_4. The Cape Grim (CG) air archive contains trace gas records known to be representative of unpolluted Southern Hemispheric air

and so provides excellent records of globally-relevant tropospheric growth rates (O'Doherty et al., 2014, and references within). UEA trace gas analysis of the CG air archive has been well documented in previous publications, for example Fraser et al. (1999) and Laube et al. (2013). Briefly, analysis is performed using a manual cryogenic extraction and pre-concentration system built in-house and connected to an Agilent 6890 gas chromatograph and a high-sensitivity tri-sector mass spectrometer. Full details of the analytical system can be found in Laube et al. (2010a, 2016). Of note is the instrument change detailed in Laube et al. (2016), whereby C_2F_6 precision is improved by analysing samples on a KCl-passivated Al PLOT column, alongside measurements of SF_6, C_3F_8, CHF_3, HFC-125, and HFC-227ea with an Agilent GS GasPro column. Prior to 2006, analysis was performed on a previous version of the analytical system (still using a GasPro column) that also used different air standards. Data analysed on this older instrument were incorporated into the time series using standard intercomparisons and standard-to-sample ratio comparisons and showed no significant differences. The ions used to quantify the gases measured at UEA were $C_2F_5^+$ (m/z 118.99) for C_2F_6, SF_5^+ (m/z 126.96) for SF_6, $C_3F_7^+$ (m/z 168.99) for C_3F_8, CHF_2^+ (m/z 51.00) for CHF_3, C_2HF_5+ (m/z 101.00) for HFC-125 and $C_3HF_7^+$ (m/z 151.00) for HFC-227ea.

These measurements have been published either as time series or as comparisons to other long-term datasets for SF_6 (Laube et al., 2013), C_2F_6 (Trudinger et al., 2016), C_3F_8 (Trudinger et al., 2016; Ray et al., 2017), CHF_3 (Oram et al., 1998) and HFC-227ea (Laube et al., 2010a; Ray et al., 2017). UEA HFC-125 has not been published previously, but the UEA data agree very well with the CG observations made by AGAGE (Advanced Global Atmospheric Gases Experiment; see website link above; data not shown). Data from high-frequency in situ and archived CG air samples measured by the Scripps Institution of Oceanography (SIO) and the AGAGE network have also been provided for CF_4, C_2F_6 and SF_6. These samples were analysed on a Medusa gas-chromatographic system with cryogenic pre-concentration and mass spectrometric detection (Arnold et al., 2012; Miller

et al., 2008). SIO CG CF_4 and C_2F_6 time series have previously been published in Mühle et al. (2010) and Trudinger et al. (2016) and their SF_6 time series in Rigby et al. (2010). SIO CF_4 and SF_6 data are reported on the SIO-05 scale and C_2F_6 on the SIO-07 scale (Mühle et al., 2010; Prinn et al., 2000).

To ensure the suitability of the CG measurements as a record of stratospheric inputs we first compensated for the time lag between observed concentrations in the Southern Hemisphere and the tropical upper troposphere – the main stratospheric input region – by applying a 6-month time shift to all CG records. The efficacy of this treatment was verified by comparing the offset CG trends to tropical (20° N to 20° S) mid- to upper-tropospheric aircraft data obtained from interhemispheric flights by the CARIBIC[2] observatory (Fig. 1). As can be seen in Fig. 1, there are some gaps in the UEA CG time series. To smooth the temporal distribution a polynomial fit was applied to each dataset and the equation from this fifth-order (CHF$_3$, HFC-125, HFC-227ea) or sixth-order (SF_6, C_2F_6 or C_3F_8) polynomial fit was used to interpolate monthly mixing ratio values. The fit was applied to the central section of each time series only (see Fig. 1) to avoid periods with significantly different growth rates; for example, there was no significant growth for HFC-125 until the mid-1990s. This central section still covered between 81 and 92 % of the UEA CG record for all compounds except CHF$_3$ (58 %) and HFC-125 (43 %) and provided a suitably long time series leading up to the stratospheric campaigns (black vertical lines in Fig. 1) for AoA calculations. We were left with a time series between 13 and 21 years long (compound dependent), which compares well to the 10- to 15-year time periods utilised in some previous studies (Engel et al., 2002, 2006; Stiller et al., 2008). A bootstrap procedure, outlined below, was used to determine whether polynomial fits were robust throughout the time period of interest. Two other fit procedures were compared to the polynomials using Igor Pro software. The cubic spline interpolation failed to cope with the temporally patchy nature of the UEA CG time series and the smoothing spline interpolation provided similar results to the polynomial fits, without the ability to incorporate them into the bootstrap procedure required for our uncertainty analysis. The mean ages derived from the fit-interpolated data were also compared to those derived from the "raw" CG time series, as used in Laube et al. (2013). The difference between the mean ages derived from these two methods was, for all compounds except HFC-227ea, a maximum of around 2 months (Supplement Sect. S2, Table S1), but the uncertainties associated with the fit-derived

mean ages was smaller than those derived from the raw CG dataset (Table S1). As the SIO CG records had a higher sampling frequency during the period of interest, only their raw time series – not fitted datasets – were used as inputs into the AoA routine.

Stratospheric measurements used in this paper were obtained from balloon- and aircraft-based whole air sampling campaigns that took place between 1999 and 2016 (Table 2). The campaigns covered the polar (B34, K2010 and K2011), mid-latitude (OB09, SC16) and tropical (B44) stratosphere. For B44, OB09, K2010, K2011 and SC16 all compounds except CF$_4$ were analysed at UEA on the same system used to analyse the tropospheric trends with B34 C_2F_6 samples being analysed on the older version of this instrument. B34 SF_6 data were provided by the Goethe University Frankfurt. Sample collection and campaign details for OB09, K2010 and K2011 are discussed in Laube et al. (2013) and OB09 and B44 are discussed in Laube et al. (2010a). The B34 campaign used the same equipment outlined in B44. For more information on the recent StratoClim campaign (SC16) visit http://www.stratoclim.org.

A subset of K2010 and K2011 samples were also analysed at SIO using the Medusa system and calibration scales described above for the AGAGE SIO CG records. SIO provided data for CF$_4$, C_2F_6 and SF_6. Due to the low pressure and volumes of these samples, only around 280 mL of sample were measured, alternated by the same volume of reference gas. The K2010 samples were at a pressure that allowed for analysis via the standard Medusa method (see references above) using Veriflow clean pressure regulators to sample 6–12 repeated measurements at roughly constant pressures. Due to the lower pressure in the K2011 samples these were analysed against an identically constructed sample flask containing a reference gas at the same pressure as the starting pressure in each K2011 sample. This allowed for both the sample and reference gas to be analysed without a regulator and allowed for concurrent pressure decreases in the sample and calibration flask, mitigating the possible impact that large differences in pressure between the ambient and calibration samples may have had on the SIO analysis. Between 3 and 8 repetitions were conducted for the K2011 samples. Analytical precisions for SIO data are provided in Table 2.

Uncertainties provided for all UEA measurements are a combination of the analytical precision calculated from repeat analyses of the calibration standard across each analysis day and the regular (usually daily) paired or triplicate analysis of individual samples. Samples for which the total uncertainty was greater than 3 times the standard deviation of the uncertainties across the entire campaign analysis period were excluded. The percentages of samples removed across all campaigns were ∼ 4 % for SF_6, CHF$_3$ and HFC-227ea, ∼ 3 % for HFC-125, 2 % for C_3F_8 and none for C_2F_6. Datasets provided by other institutions (University of Frankfurt B34 SF_6 and SIO K2010 and K2011 data) were smaller

---

[2]CARIBIC (Civil Aircraft for the Regular Investigation of the atmosphere Based on an Instrument Container), part of IA-GOS (www.iagos.org), is an observatory based on approximately monthly flights on-board a commercial Lufthansa Airbus A340-600 from Frankfurt to destinations on several continents. Further details can be found at http://www.caribic-atmospheric.com/.
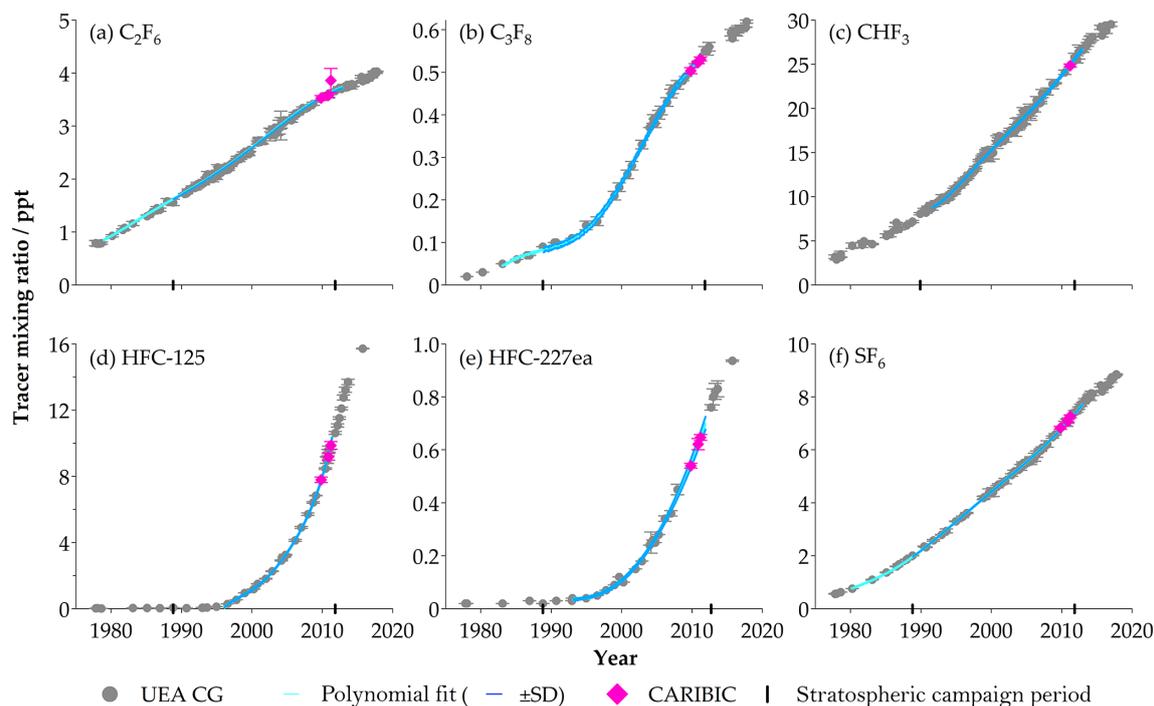
Figure 1. UEA CG time series (6-month time shift), polynomial fits applied to these time series and associated errors (see inset legend). Details of the analytical uncertainties in UEA CG time series, application of polynomial fit and comparison with CARIBIC data are provided in Sect. 2. Vertical black lines on the *x* axis show the section that contains the 10-year period leading up to each of the stratospheric campaigns used during the bootstrap procedure (Sect. 3(a)).

Table 2. Overview of stratospheric campaigns used in this study.

Abbreviation	Campaign dates	Platform	Location, altitude*, latitude, longitude, campaigns, collaborations	Data availability: where data are available for individual campaigns the percent of analytical precision is given.						
				CF$_4$	C$_2$F$_6$	C$_3$F$_8$	CHF$_3$	HFC-125	HFC-227ea	SF$_6$
B34	6 Feb 1999	High-altitude balloon-borne whole air sampler	Kiruna, Sweden Up to 26 km, 62–77° N, 1° W–29° E		1.8					2.1
B44	11 Jun 2008		Teresina, Brazil Up to 33.5 km, 5° S, 43° W Launched by the French Space Agency, Centre National d'Etudes Spatiales		2.4				3.1	1.5
OB09	30 Oct 2009 4 Nov 2009	M55 Geophysica high-altitude aircraft	Oberpfaffenhofen, Germany 10–20 km, 48–54° N, 7–12° E		0.8			0.3	1.6	0.5
K2010 UEA	20 Jan 2010 and		Kiruna, Sweden 9–19 km, 62–77° N, 1° W–29° E		0.4	1.1	1.4	0.7	1.5	0.7
K2010 SIO	2 Feb 2010		Part of RECONCILE (von Hobe et al., 2013) and ESSENCE campaigns		0.3	2.0				1.4
K2011 UEA	11 Dec 2011 and				1.5		0.6		1.1	1.2
K2011 SIO	16 Dec 2011			0.4	2.5					1.3
SC16	1 Sep 16 and 6 Sep 2016		Kalamata, Greece 10–21 km, 33–41° N, 22–32° E Part of EU StratoClim project	0.7	1.3	0.5	1.0	0.8	0.8

* Maximum sampling altitude for balloons and cruising altitude range for aircraft.

and could therefore not be quality controlled in this manner; all data provided to us were included in further analyses.

A sample of stratospheric air represents a mixture of air masses with different transport histories and thus different ages. This distribution of transport times is the "age spec-trum", a probability density function for which the first moment, or mean, is the mean age for that parcel and the second moment, or variance, is the width of the age spectrum (Hall and Plumb, 1994). Mean ages were calculated using the method described in Engel et al. (2002) based on the method

provided for inert tracers by Hall and Plumb (1994). This method has been further discussed and modified in various publications, including Engel et al. (2006, 2009), Bönisch et al. (2009) and Laube et al. (2013). Where we use or refer to the methodological tests or variations used in the papers subsequent to Engel et al. (2002) we will reference these explicitly. To calculate mean age, one requires a tropospheric trend, stratospheric measurements and an understanding of the width of the age spectrum. As this study focuses on assessing potential new age tracers we carefully considered the uncertainties associated with the mean ages calculated by our AoA routine. This uncertainty analysis is described in Section 3, where we consider the uncertainties associated with the main inputs to the AoA routine.

3   Description of and results from the age tracer uncertainty assessment

As this study focuses on assessing potential new age tracers we carefully consider the uncertainties associated with the mean ages calculated by our AoA routine. Potential sources of uncertainty include

a.   uncertainties in the tropospheric trend,

b.   uncertainties in the stratospheric measurements,

c.   different methods of implementing the tropospheric trend within the AoA routine, and

d.   different methods for the parameterisation of the width of the age spectrum.

These four main areas of uncertainty are discussed below. A wider suite of tests was performed to help us better understand the mean age uncertainties, many of which have informed our protocol for investigating the main uncertainty components (a–d) or are referenced in our analysis of these components in the following text. Section S2 includes a table (Table S1) which provides an overview of the full suite of uncertainty tests performed on our dataset.

For each uncertainty analysis a similar procedure was followed. Here the procedure is outlined using generic terminology, with a specific example for each step as used in our study.

1. *Task.* A component of the mean age calculation was identified and considered as the base scenario. *Example.* We used our Cape Grim raw time series (the grey markers in Fig. 1) as the tropospheric trend input.

2. *Task.* The errors associated with this component were identified. *Example.* In our case this means the analytical uncertainty in each of the measurements in the raw time series.

3. *Task.* A "min" and a "max" dataset was created using these uncertainties. Our mean mixing ratio minus the respective analytical uncertainty value provides the "raw_min" dataset. *Example.* The addition of the analytical uncertainty provides "raw_max".

4. *Task.* A mean age is calculated for each of our stratospheric air samples using the base scenario. *Example.* Our mean ages were calculated using "raw" as the tropospheric input.

5. *Task.* Keeping everything else constant (Table S1) the mean age was calculated again using the "min" and "max" datasets. *Example.* Our mean ages were calculated using "raw_min" and "raw_max" as tropospheric inputs.

6. *Task.* The mean ages obtained from "min" and "max" are compared to those from the base scenario. In our case, the differences between the "min" and "max" cases are often plotted as a "residual plot". The average difference between the "min" and "max" cases is provided in Table 3 (if one of the key uncertainties) or Sect. S2 (all tests). *Example.* The mean ages derived for each stratospheric measurement using "raw", "raw_min" and "raw_max" are compared. The absolute average difference between "raw" and its min–max variants was 0.5 months for SF_6 (case 2 in Table S1).

(a) Uncertainties in the tropospheric measurements

The first class of uncertainties we consider are those associated with the fit-interpolated tropospheric trend (cases 4 and 5 in Table S1). Here our base scenario is comprised of mean ages derived from the fit-interpolated tropospheric trend (hereafter referred to as "fit") compared to those derived from "fit_min" and "fit_max", which we obtained from a bootstrap procedure (Efron, 1979; Singh and Xie, 2008). No sampling perfectly represents natural variability and the resampling procedure used during the bootstrapping is designed to provide an indication of the impact of this "subsampling effect". Our bootstrap procedure was performed as follows.

1. To enhance our representation of atmospheric variability, we first took our CG time series (Table 1) and converted it to a $3n$ dataset comprised of [original_data] + [original_data_minus_analytical_uncertainty] + [original_data_plus_analytical_uncertainty]. However, we only resampled a dataset of the original size.

2. We used the bootstrap macro for Microsoft Excel provided by Barreto and Howland (2006) to resample (with replacement) our CG dataset. A polynomial fit was applied to each resample.

Table 3. Uncertainties* associated with calculating the mean age of air for stratospheric samples.

Compound	±uncertainties as monthly mean (min–max)				
	(a) Tropospheric trend uncertainties	(b) Stratospheric measurement uncertainties	(c) "Quadratic" vs. "convolution" AoA routines	(d) Uncertainty in parameterisation of width of age spectrum	Combined uncertainty (a + b only)
CF_4 SIO	2.1 (1.2–2.5)	4.7 (2.3–8.6)	–	–	–
C_2F_6	1.8 (1.6–2.2)	5.8 (2.1–10.6)	0.6 (<0.1–1.0)	0.7 (0.1–1.2)	6.0 (2.8–10.6)
C_2F_6 SIO	4.2 (3.5–5.1)	11.1 (3.6–20.2)	–	–	–
C_3F_8	2.5 (1.9–4.3)	3.2 (1.1–6.8)	1.0 (0.4–1.3)	0.7 (<0.1–1.0)	3.7 (2.5–7.2)
CHF_3	1.5 (1.3–1.7)	4.5 (0.3–10.7)	0.1 (<0.1–0.2)	0.3 (<0.1–0.5)	4.9 (1.4–10.7)
HFC-125	0.6 (<0.1–0.8)	0.6 (<0.1–1.2)	0.6 (<0.1–1.2)	0.5 (<0.1–1.4)	0.9 (0.3–1.4)
HFC-227ea	2.4 (1.8–3.2)	2.9 (0.4–15.4)	0.2 (<0.1–0.9)	0.4 (<0.1–1.4)	4.2 (2.2–14.3)
SF_6	1.1 (0.4–1.9)	2.5 (<0.1–7.0)	0.2 (<0.1–0.7)	0.3 (<0.1–0.5)	2.8 (1.1–7.0)
SF_6 SIO	1.6 (1.3–5.0)	2.8 (1.3–6.5)	–	–	–

*These are averages from campaigns B44, OB09, K2010 and K2011 (Table 2). B34 data are not included as the analysis of these samples was performed on an older instrument (C_2F_6) or not at UEA (SF_6). SC11 data are not included as a full uncertainty analysis was not performed on SC16 due to the complex air sample source region (Sect. 4).

3. After 1000 iterations, the standard deviation of the fit parameters was calculated.

4. The standard deviation from the bootstrapping procedure was used to create "fit_min" and "fit_max" datasets which could be used as tropospheric inputs to the AoA routine.

The ±1 standard deviation uncertainties from this procedure are plotted as dark blue lines in Fig. 1. The uncertainties associated with the fits are small and show that the polynomials are robust throughout the section of the trend used as an input into the AoA routine. The mean ages resulting from "fit_min" and "fit_max" were compared to the original mean age values to give an uncertainty estimate for the tropospheric trend components of the AoA routine (Table 3). Average uncertainties were around 1–3 months. There are some higher values for C_3F_8 and HFC-227ea due to the poorer data coverage in the late 2000s causing the fit to be slightly less robust. This highlights the importance of ongoing, reliable and regular tropospheric time series measurements for potential new age tracers. These uncertainties will be combined into an overall uncertainty for each species later in the paper.

(b) Uncertainties in the stratospheric measurements

As with the tropospheric trends, "stratmin" and "stratmax" datasets based on our measurements ± the analytical uncertainties were used as inputs into the AoA routine and the outputs compared to mean ages derived from the original stratospheric mixing ratios (cases 8 and 9 in Table S1). Results from this comparison are shown as a residual plot in Fig. 2, in which the residuals are the differences between the mean age calculated using our original stratospheric mixing ratios and those from "stratmin" and "stratmax". The impact of the stratospheric measurement uncertainty is larger than for the

tropospheric inputs: roughly double for CF_4, C_2F_6, CHF_3, HFC-227ea and SF_6 and similar for C_3F_8 and HFC-125, but generally averaged around half a year or less for all compounds (Table 3). Differences between different compounds can be attributed to a combination of their growth rates and their stratospheric measurement precision (Table 2). The ratio of the stratospheric measurement precision to the growth rate impacts our mean age resolution: uncertainties derived from our stratospheric measurement precision will be greater if the growth rate is smaller. The growth rate of C_2F_6 was slowing (Fig. 1) in the period leading up to our 2009–2011 campaigns and this contributes to the larger uncertainties associated with C_2F_6 compared to other compounds, despite similar analytical precisions (Table 2). For C_2F_6 and SF_6 there are both UEA and SIO values (Fig. 2; cases 35 and 36 in Table S1). The mean ages derived from stratospheric samples analysed by SIO are independent of the UEA measurements, having been calculated using AGAGE-based tropospheric trends and uncertainties. There are some higher SIO C_2F_6 residual values linked to the higher analytical uncertainty for the SIO measurements (Table 2). This increased uncertainty is not unexpected: C_2F_6 is the least abundant of the three gases measured by SIO for this study and their analytical system is designed for air samples an order of magnitude, 2 L versus 280 mL, larger than what is available from stratospheric samples. SF_6 measured at both UEA and SIO showed similar stratospheric uncertainties. Independent verification adds significant weight to the suitability of these new compounds for use as age tracers. The larger impact of uncertainties in stratospheric data compared to the tropospheric trend (Table 3) highlights the importance of precise measurements of these compounds if they are to be suitable age tracers. These stratospheric uncertainties are combined with uncertainties from Sect. 3(a) to create an overall uncertainty later in the paper.
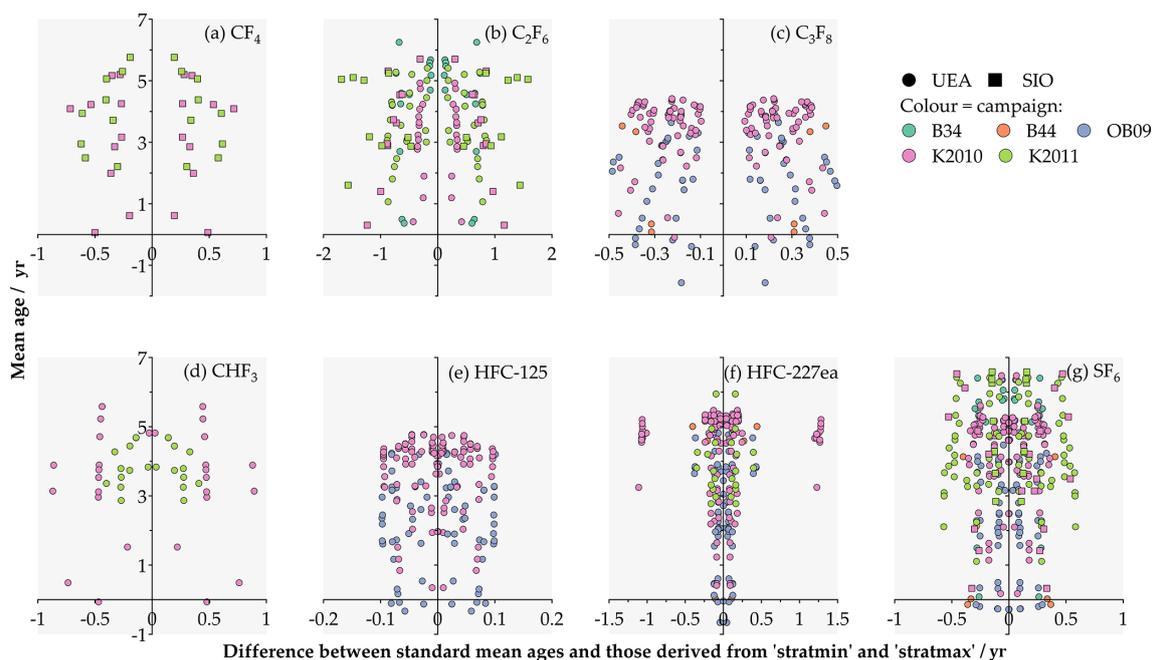
Figure 2. Residual plots showing the uncertainties associated with varying the stratospheric measurement inputs for the AoA routine. The x axis shows the difference between the mean ages calculated using a minimum and maximum stratospheric mixing ratio compared to using the mean mixing ratio normally used, the mean age of which is on the y axis (Sect. 3(b); cases 8 and 9 in Table S1). The marker shape denotes which institution performed the analysis and the marker colour the stratospheric campaign; see inset legend. The vertical axis labels for each row are in the left panel.

(c) Comparing different methods for implementing the tropospheric time series component of the mean age calculation

One limitation of the AoA routine used in this study is that only a quadratic function can be used when fitting the tropospheric time series for the AoA calculation. A recent improvement is to calculate AoA by using a numerical method that uses the convolution of the age spectra approximated by an inverse Gaussian distribution with the tropospheric time series (Ray et al., 2017), which overcomes the limitations of a quadratic fit to approximate such trends. We implemented this numerical convolution method in our AoA routine so that we could compare mean ages derived from our data using both the original quadratic and the numerical convolution algorithms (case 18 in Table S1). The resulting "residual plot" can be seen in Sect. S3 and the average uncertainties in Table 3. We found that outside of very young (< 1 year) mean ages the difference between these two methods was 1 month or less. The weaker performance near the tropopause is a known problem of the convolution method for younger mean ages, which require the convolution over a short time period, potentially leading to mean age biases due to observed short-term variability and/or data sparsity. As the quadratic method performed better across the whole range of mean ages in our study, we use that method to derive mean ages and uncertainties discussed in all subsequent sections of the paper.

(d) Uncertainty in parameterisation of width of age spectrum

As described in Engel et al. (2002), stratospheric mixing ratios cannot simply be calculated by propagating the tropospheric trend into the stratosphere: due to non-linearities in the tropospheric trends for our compounds of interest, the width of the age spectrum impacts the propagation of these trends. As the width of the age spectrum cannot be measured directly, we assume a constant value of 0.7 as the parameterisation of the ratio $\frac{\text{width age spectrum}^2}{\text{mean age}}$ (from Hall and Plumb, 1994, as used in Engel et al., 2002 and Laube et al., 2013). Previous studies have investigated the effect of varying this parameterisation. Engel et al. (2002) investigated the impact of using values of 0, 0.7 and 1.25 and found differences of less than half a year for CO_2 and SF_6 mean ages. They also reported that the best agreement between these two age tracers was reached when using 0.7. Laube et al. (2010b) also tested the impact of this value on calculated fractional release factors (FRFs; see Sect. 5), comparing values of 0.5, 0.7 and 1.25, and found that this factor had a small impact on the FRF for a range of long-lived halocarbons. As this study introduces new potential age tracers, investigating the impact of this parameterisation is pertinent. Values of 0.5 and 1 were compared to the commonly used value of 0.7 (residual plot in Sect. S3). The results are shown in Table 3: one can see

that the impact is small (< 1 month on average) compared to the impact of (a) and (b) and is similar for all compounds.

## 4 Combination of errors and analysis of new age tracers

The two key uncertainties from Sect. 3, namely those associated with the tropospheric trend and stratospheric measurements (columns a and b in Table 3), were combined and used as the error bars in Fig. 3, which shows a vertical profile of the mean ages derived from all six of our tracers. We use CFC-11 instead of height or potential temperature as a vertical coordinate because it has a well-quantified vertical distribution (Hoffmann et al., 2014) influenced by the same localised transport and mixing processes as our observed age tracers. Tropospheric CFC-11 mixing ratios have slowly declined in the period covered by the stratospheric campaigns (1999–2011) at a rate of between 0.5 and 1 % per year (based on our CG trend). A linear fit of the data throughout this period was relatively robust: ~ 3 % standard deviation between fits calculated over eight different time windows and R^2 values of > 0.99 for all eight fits. Based on this we corrected the CFC-11 mixing ratios for the stratospheric campaigns relative to the earliest (B34 in 1999) campaign. This is a simplification, as the propagation of tropospheric mixing ratios into the stratosphere is influenced by the width of the age spectrum (see Sect. 2). As the CFC-11 mixing ratios are not used in further calculations (purely as a visual indicator of altitude) and the trend during the time period covered is linear and small, we felt it a suitable approximation for our needs.

As mentioned before, a suitable age tracer must have a well-quantified, monotonically changing tropospheric trend, precise stratospheric measurements and be relatively inert in the stratosphere. The suitability of our new age tracers to meet the first two requirements is shown by the error bars in Fig. 3 and the final column in Table 3. The uncertainties of the new age tracers were compared to those associated with SF_6 and were found to be similar for C_3F_8 and HFC-227ea, smaller for HFC-125 and larger but within a similar magnitude range for CF_4, C_2F_6 and CHF_3. In this respect, these new age tracers are as suitable as the commonly used tracer SF_6. As for the final point, that the compounds are inert in the stratosphere (suggested by their lifetimes; see Table 1), this is also supported by Fig. 3 in which we can compare the mean ages derived from the new tracers to those derived from SF_6. It is interesting that SF_6 (current lifetime estimate 3200 years) lies to the right of the plot, the trend line in Fig. 3a overlapping with HFC-227ea (stratospheric lifetime estimated at 673 years). This high bias in SF_6-derived mean ages supports the recently revised SF_6 lifetime estimate of 850 (580–1400) years (Ray et al., 2017). The other compounds tend to give younger mean ages consistent with longer stratospheric lifetimes. In particular, HFC-125 shows evidence of having a stratospheric lifetime well in excess of

351 years (see Sect. 1). Loss of SF_6 may be understandable in the polar regions during winter due to the mesospheric sink and the downward transport of SF_6-depleted mesospheric air within the polar vortex, but when we split our results into polar (Fig. 3b) and mid-latitude and tropical (Fig. 3c) flights one can see that the SF_6 fit still mimics that of HFC-227ea, suggesting that there is evidence even in this region that SF_6-derived mean ages may be more consistent with the shorter-lived HFC-227ea. This raises the question as to whether the sink of SF_6 is indeed exclusively located in the mesosphere, although admittedly our non-polar dataset is limited and we cannot rule out mixing of polar vortex air (or vortex remnants) being observed in mid-latitudes outside of the winter polar vortex (Strunk et al., 2000).

Table 4 shows the degree of agreement within stratospheric measurement uncertainties (column b in Table 3) of the mean ages derived from each of the age tracers. There is strong agreement between all the new age tracers: CF_4, C_2F_6, C_3F_8, CHF_3 and HFC-125. Mean ages derived from these compounds, except for CHF_3, do not agree well with the mean ages derived from SF_6 and HFC-227ea. With the lifetime of CHF_3 in the middle of our range of tracer lifetimes (Table 1) we would expect CHF_3-derived mean ages to agree with both shorter- and longer-lived compounds. There is good agreement between HFC-227ea and SF_6. Table 4 also shows the degree of agreement when the data are split into polar and mid-latitude and tropical datasets. There are fewer data for the latter group for which we have co-measurements of two or more age tracers. However, there is still good evidence that the agreement between SF_6 and HFC-227ea is stronger than for SF_6 and the new age tracers.

We combined the results from the new age tracers (CF_4, C_2F_6, C_3F_8, CHF_3 and HFC-125) to derive a new "best estimate" of the mean age of air and plotted this against the SF_6 mean age in Fig. 4. As we may expect different results in the tropics, the input region to the stratosphere, we have removed our four tropical measurements from our dataset and this slightly reduced dataset is listed as "all (no tropical)" hereafter. A bivariate linear regression is included for the whole (no tropical) dataset. Bivariate regression fits using only polar, mid-latitudinal or tropical data (also in Fig. 4) do not result in significantly different slopes (although the tropical fit exhibits large uncertainties as it is based on four points only). Both Figs. 3 and 4 show that the agreement between SF_6 and the other tracers weakens for older mean ages. This is similar to the relationship between mean ages derived from CO_2 and SF_6, which has been shown to be "excellent" for mean ages up to 3 years by Andrews et al. (2001) and to agree within errors (within a < 0.6-year difference) with Engel et al. (2002). Interestingly, although we do not have CO_2 data for our campaigns, the slope in Fig. 4 is remarkably similar to the $\sim 0.8 : 1$ slope derived by Andrews et al. (2001), who compared mean ages of air derived via SF_6 and CO_2. Within our "all (no tropical)" dataset, our best-estimate mean age agreed within uncertainties with the SF_6-derived mean age
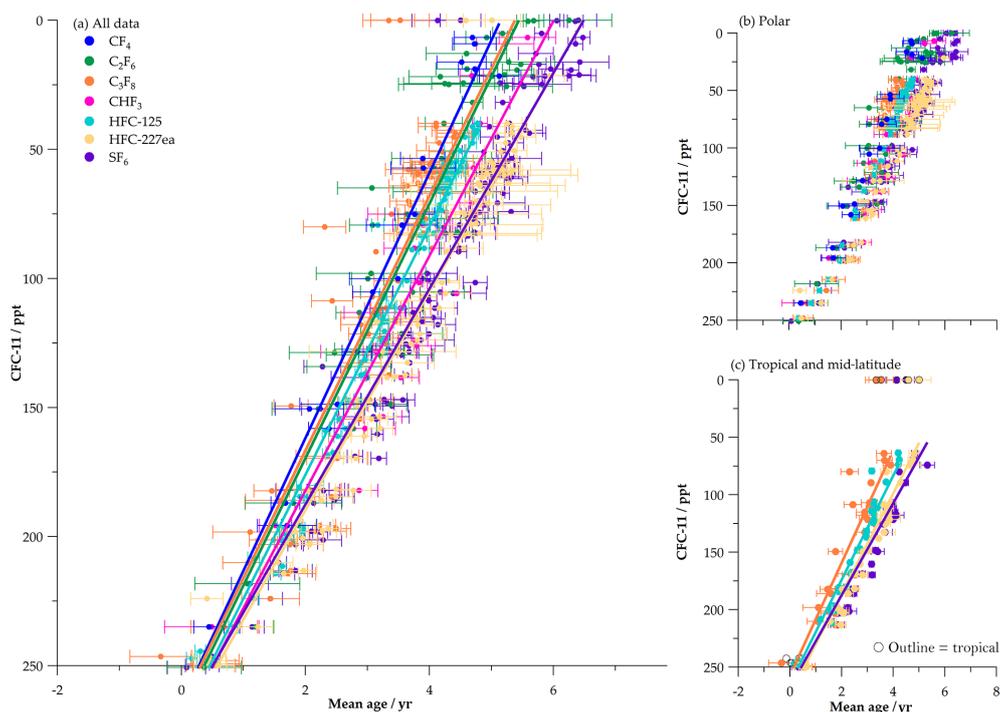
Figure 3. Vertical profiles of mean ages derived from all compounds used in this study. Panels **(b)** and **(c)** show the same data as in **(a)** but split into polar **(b)** and mid-latitude and tropical **(c)** flights only (see Table 2 for campaign details). Colours represent different age tracers (see inset legend) and remain the same across all panels.

Table 4. Percentage of samples for which the mean age derived from two tracers agreed within the uncertainties*.

	Percentage agreement							Number of samples with measurements of both compounds						
	CF4	C2F6	C3F8	CHF3	HFC-125	HFC-227ea	SF6	CF4	C2F6	C3F8	CHF3	HFC-125	HFC-227ea	SF6
All data														
CF4		93		77		40	35		15	6	13	5	10	17
C2F6				93			56			9	14	8	9	48
C3F8				76		46	34				9	91	92	92
CHF3						84	70					8	19	23
HFC-125						32	15						87	88
HFC-227ea							89							98
SF6														
Mid-latitude and tropical data														
CF4									0	0	0	0	0	0
C2F6										0	0	0	0	0
C3F8				76		50	46				0	33	34	37
CHF3												0	0	0
HFC-125						47	27						30	33
HFC-227ea							82							33
SF6														
Polar data														
CF4		93		77		40	35		15	6	13	5	10	17
C2F6				93		56	56			9	14	8	9	48
C3F8				76		43	25				9	58	58	55
CHF3						84	70					8	19	23
HFC-125						26	7						57	55
HFC-227ea							92							65
SF6														

Shading bands:
0–20 %
20–40 %
40–60 %
60–80 %
80–100 %

63 % of the time for mean ages < 4 years, 42 % of the time within the Engel et al. (2002) window of 2–5 years and only 16 % of the time above 5 years. Our results suggest that care should be taken when using SF6 as an age tracer for older (high-altitude) air where its loss processes (Sect. 1) may bias derived mean ages. The smaller sample size with mean ages less than 3 years ($n = 33$ compared to $n = 112$ over 3 years) makes it difficult to conclude if this bias exists in samples with SF6-derived young mean ages. However, Fig. 4 shows that when the fit is applied only to samples with SF6 mean ages < 3 years, it is for the most part similar (within uncertainties) to that derived from the complete dataset.

Figure 4 also includes SC16 data from recently analysed mid-latitude data from two aircraft flights in the Mediterranean region (Table 2). Stratospheric uncertainties (as outlined in Sect. 3(b)) were calculated for SC16 samples in the
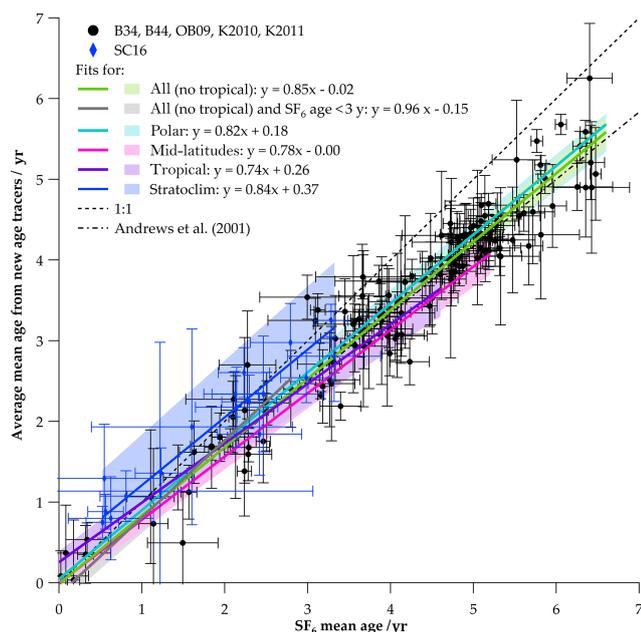
Figure 4. "Best-estimate" mean ages (a combined mean age based on CF_4, C_2F_6, C_3F_8, CHF_3 and HFC-125) plotted against SF_6 mean age. Error bars are based on stratospheric uncertainties from Table 3 column b. All fits are bivariate linear fits with uncertainties shown by shaded areas (see inset legend). SF_6 vs. CO_2 line from Andrews et al. (2001) included for comparison.

same manner as for other compounds. As our existing selection of high-altitude campaigns only included two mid-latitude and one tropical flight (the latter comprised of only four data points) we thought it important to include these data. However, the SC16 samples are not discussed in the error analysis above for two reasons. Firstly, the target of this campaign was to sample polluted air from the Asian monsoon outflow. The impact of pollution can be seen in the high levels of several gases, including SF_6, near the tropopause (all but three samples were collected at potential temperatures > 380 K). Secondly, the estimation of mean ages near the tropopause is limited by the availability of our CG-based tropospheric trend, which currently ends in February 2017. As that trend needs to be shifted by 6 months to account for interhemispheric transport (see Sect. 2) it only just extends to the time of these flights, increasing the uncertainties associated with the polynomial fits (Sect. 2). As high levels of SF_6 or other age tracers biases the derived mean ages toward younger values, the more uncertain mean ages (< 0.5 years) were removed for Fig. 4 and further analysis. Despite these differences, the slope of SF_6-based vs. best-estimate-based mean ages for SC16 is similar to that of the other campaigns.

5 Implications for policy-relevant parameters

Younger mean ages do have implications for three important policy-relevant parameters that are used to quantify the impact of halocarbons on stratospheric ozone:

a. stratospheric lifetimes of ODSs;

b. FRFs (the fraction of a halocarbon that has been converted into its reactive (ozone-depleting) form in the stratosphere; compounds with larger FRFs result in greater ozone depletion); and

c. ODPs (a measure of the impact of individual halocarbons to deplete ozone relative to CFC-11).

In Laube et al. (2013) these three parameters were calculated using SF_6-based mean ages. Here we revisit the Laube et al. results and calculate updated FRFs, lifetimes and ODPs using our new best-estimate mean age derived from our five new age tracers for the following 10 ODSs: CFC-11, CFC-113, CFC-12, HCFC-141b, HCFC-142b, HCFC-22, Halon-1301, Halon-1211, carbon tetrachloride (CCl_4) and methyl chloroform (CH_3CCl_3). CFC, halon and HCFC formulas are given in Table 5. We also compare these results to the WMO (2014) recommendations.

5.1 Stratospheric lifetimes derived from new age tracers

The lifetime of the 10 ODSs listed above were calculated in Laube et al. (2013) using a method dependent on the slope of the correlation between CFC-11 mixing ratios and mean ages at the tropopause. When using the new best-estimate mean age this slope changes from -20.6 ± 4.6 to -28.6 ± 4.3 ppt yr^{-1}. The updated stratospheric lifetimes calculated from our new slope are shown in Table 5 alongside the old values and recommendations from WMO (2014). In WMO (2014) the stratospheric lifetimes are taken from model mean values (with the exception of CCl_4, for which they used tracer and model mean data) from SPARC (2013). As our lifetime calculation only produces lifetimes relative to that of CFC-11, changes are generally small. The exceptions are the three main hydrochlorofluorocarbons (HCFCs), for which the lifetime has decreased significantly compared to Laube et al. (2013), and CH_3CCl_3 for which it has increased. Both changes bring our estimations closer to those of WMO (2014). This is linked to the relatively large changes (increases for HCFCs and a decrease for CH_3CCl_3) in the tropospheric abundances of these gases in recent years.

5.2 Fractional release factors derived from new age tracers

Two updates to the calculations of FRFs reported in Laube et al. (2013) were made, and the resulting FRFs can be seen in Table 6 alongside the original Laube et al. results and

Table 5. Updated stratospheric lifetimes based on "best-estimate" mean ages derived in this study compared to existing literature values.

Compound	Formula	Stratospheric lifetime* (yr) (min–max)*		
		This study	Laube et al. (2013)	WMO (2014)
CFC-11	$CFCl_3$	60 (54–67)	60 (54–67)	–
CFC-113	$CF_2ClCFCl_2$	83 (75–94)	82 (74–93)	88.4
CFC-12	CF_2Cl_2	(102)	(100)	95.5
HCFC-141b	CH_3CFCl_2	101 (64–221)	122 (70–454)	72.3
HCFC-142b	CH_3CF_2Cl	178 (103–459)	406 (139–∞)	212
HCFC-22	CHF_2Cl	129 (94–204)	184 (113–647)	161
Halon-1301	CF_3Br	78 (72–85)	82 (75–93)	73.5
Halon-1211	CF_2ClBr	37 (32–42)	36 (32–41)	41
CCl_4	CCl_4	53 (46–63)	53 (45–62)	44
CH_3CCl_3	CH_3CCl_3	37 (26–52)	30 (21–43)	38

* All lifetimes calculated using CFC-11 lifetimes of 60 years, with CFC-11 lifetimes based a on CFC-12 lifetime of 100 (Laube et al., 2013) or 102 (this study) years.

WMO (2014) values based on observation-based FRFs from Newman et al. (2007). The first change was to use our new best-estimate mean age in the FRF calculation. The second change was to use the new methodology outlined in Oster-möller et al. (2017). Plumb et al. (1999) presented a new formula to calculate FRFs that considers the dependency of the age spectrum on the stratospheric lifetime and tropospheric trend of the ODS in question. We applied this correction using the exact parameterisation suggested by Plumb et al. (1999). We note that some of the lifetimes used by Plumb et al. are somewhat different to ours, but tests on the influence of lifetime on FRFs derived from this parameterisation showed that the impact was limited to ±0.03, which is well within our FRF uncertainties (Table 6). Changes from the initial mean age correction are significant and would result in increased FRFs throughout. However, these two corrections can have contrary effects for species with strongly increasing (e.g. HCFC-22; Fig. 5b) or decreasing (CH_3CCl_3; Fig. 5c) tropospheric abundances. For HCFC-22 the two corrections work in the same direction, resulting in substantially higher FRFs at a given mean age. For CH_3CCl_3 the opposite is true and we see very little change.

5.3 Ozone depletion potentials derived from new age tracers

ODPs were calculated relative to CFC-11 using the method in Laube et al. (2013) but with updated tropospheric lifetimes from WMO (2014), the latter mainly affecting compounds with significant removal in the troposphere. As ODPs were calculated relative to CFC-11 (FRF changes shown in Fig. 5a), changes to ODPs are only significant for the three hydrofluorocarbons (HCFCs), which have strong positive trends and thus the largest changes to their FRFs. Our full set of updates can be seen in Table 7. The new HCFC ODP values are now closer to the recommended values in

Table 6. Updated mid-latitude FRFs based on our "best-estimate" mean ages (taken at 3 years) derived in this study compared to existing literature values.

Compound	This study (min–max)	Laube et al. (2013)	WMO (2014)
CFC-11	0.47 (0.43–0.52)	0.35 (0.32–0.39)	0.47
CFC-113	0.30 (0.27–0.34)	0.22 (0.20–0.25)	0.29
CFC-12	0.26 (0.23–0.30)	0.19 (0.16–0.21)	0.23
HCFC-141b	0.31 (0.27–0.36)	0.17 (0.14–0.21)	0.34
HCFC-142b	0.13 (0.11–0.15)	0.05 (0.04–0.06)	0.17
HCFC-22	0.13 (0.11–0.15)	0.07 (0.05–0.08)	0.13
Halon-1301	0.39 (0.35–0.43)	0.26 (0.24–0.29)	0.28
Halon-1211	0.66 (0.61–0.71)	0.52 (0.48–0.56)	0.62
CCl_4	0.76 (0.66–0.86)	0.42 (0.39–0.46)	0.56
CH_3CCl_3	0.69 (0.64–0.75)	0.61 (0.56–0.65)	0.67

WMO (2014), and we see agreement between HCFC-141b and HCFC-22 within our uncertainties. Nevertheless, for all other ODSs except CH_3CCl_3, we still find ODPs significantly different to the ones used in WMO (2014). This is even the case when we increase our CFC-11 lifetime to 60.2 years, the equivalent of assuming a CFC-12 lifetime of 102 years as recommended in WMO (2014). However, WMO (2014) values are based on Newman et al. (2007) and do not include the recent correction by Ostermöller et al. (2017). What is also noteworthy from Fig. 5 is that the discrepancy between the FRF mean age correlations reported in WMO (2014) and Laube et al. (2013) largely disappears with our updates. This confirms the suspicion mentioned in Laube et al. (2013) that this discrepancy might predominantly arise from the use of different age tracers (WMO, 2014 used CO_2-derived mean ages).
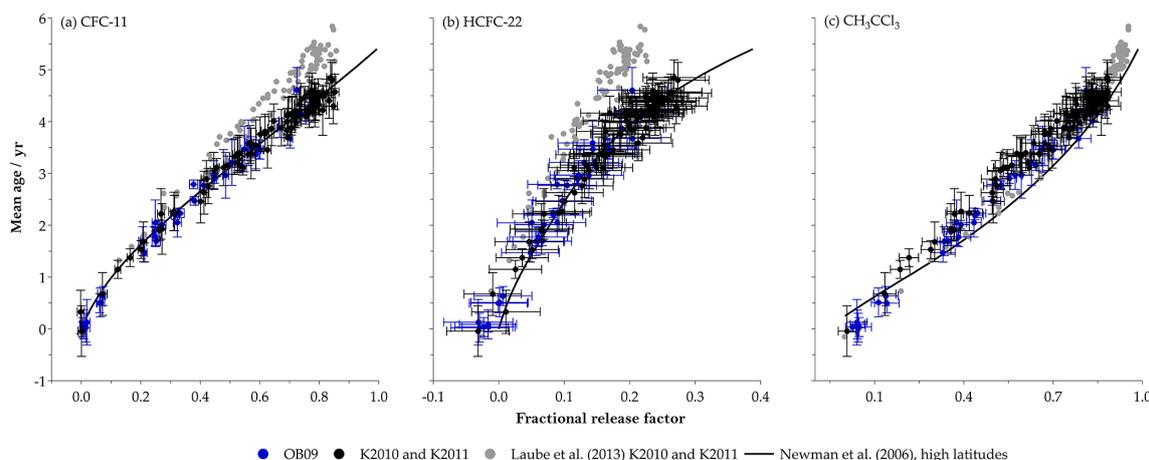
Figure 5. Changes in FRFs resulting from our new "best-estimate" mean age of air and the improved FRF calculation method from Oster-möller et al. (2017) for OB09, K2010 and K2011 compared to previously published K2010 and K2011 data (Laube et al., 2013) and FRF mean age correlations from Newman et al. (2006). Shown for three compound case studies; see details in the main text of the paper.

Table 7. Updated ODPs based on "best-estimate" mean ages (taken at 3 years) derived in this study compared to existing literature values. Numbers in brackets are min–max* values.

Compound	This study		WMO (2014)	Laube et al. (2013)
	ODP	% difference relative to WMO		
CFC-11	1, by definition	–	1	1
CFC-113	0.68 (0.61–0.76)	−20	0.81	0.63 (0.57–0.69)
CFC-12	0.70 (0.62–0.79)	−15	0.73	0.67 (0.59–0.75)
HCFC-141b	0.083 (0.069–0.10)	−18	0.102	0.063 (0.051–0.076)
HCFC-142b	0.037 (0.031–0.043)	−34	0.057	0.019 (0.015–0.025)
HCFC-22	0.028 (0.022–0.035)	−17	0.034	0.019 (0.015–0.025)
Halon-1301	19.0 (17.0–22.0)	−25	15.20	18.7 (17.0–20.3)
Halon-1211	5.51 (4.89–6.24)	−20	6.90	5.8 (5.2–6.5)
CCl_4	0.92 (0.80–1.05)	28	0.72	0.82 (0.77–0.87)
CH_3CCl_3	0.13 (0.11–0.14)	−11	0.14	0.14 (0.13–0.16)

* Min and max values derived from min and max lifetimes and FRF values from Tables 5 and 6. Based on a CFC-11 lifetime of 60 years.

6 Conclusions

We have presented tropospheric trends and stratospheric measurements of seven trace gases and evaluated their capability to estimate stratospheric mean ages, which are useful proxies for stratospheric transit times. We find that these gases have suitable tropospheric growth rates and measurement precisions ($< 2\%$ for all compounds across all stratospheric campaigns) for this purpose. A comprehensive uncertainty analysis was performed on several factors contributing to the uncertainties in tracer-derived mean ages. Uncertainties in AoA estimates based on our new tracers were approximately equal to or less than 6 months for all compounds, which are similar to those for the existing tracer SF_6. In addition, independent analysis of three gases (CF_4, C_2F_6 and SF_6) at SIO using different calibration scales and indepen-

dent tropospheric trends resulted in very similar mean ages. Importantly, five of these gases, CF_4, C_2F_6, C_3F_8, CHF_3 and HFC-125, produce very similar mean ages of air, allowing us to produce a new best-estimate mean age which we compared to SF_6-derived mean ages. Whilst our non-polar dataset is limited, we provide some qualitative evidence to suggest potential SF_6 loss outside of the polar vortex and support recent work which suggests a reduction in the SF_6 stratospheric lifetime from 3200 to 850 years (Ray et al., 2017). The discrepancy between SF_6- and best-estimate-derived mean ages is greater for older air, as seen for the CO_2–SF_6 relationship in Andrews et al. (2001), Engel et al. (2002, 2006) and Ray et al. (2017), although somewhat in disagreement with Strunk et al. (2000), who found that SF_6 and CO_2 mean ages were consistent up to mean ages of around 7–8 years. Further data

from stratospheric balloon and aircraft flights are needed to answer this question in the future.

The new tracers identified here are not meant to replace SF_6 and CO_2, which are established age tracers with well-defined tropospheric trends and a wealth of stratospheric measurements, particularly as they are measurable by satellite (Stiller et al., 2008). CO_2, in particular, also has an extremely long stratospheric lifetime. However, the fact that multiple tracers suggest that SF_6 mean ages have a high bias suggests a need for caution when using SF_6 to derive mean ages, especially above the lowermost stratosphere. We also note that, unlike CO_2, our new age tracers do not have large seasonal cycles or stratospheric sources and are therefore better suited as tracers of transport times in the lower stratosphere. As future changes to the BDC are likely to be complex, a suite of tracers may be better suited than SF_6 or CO_2 alone in diagnosing long-term changes.

Finally, we use a new tracer-derived best-estimate mean age and investigate the knock-on effects on policy-relevant parameters such as stratospheric lifetimes, FRFs and ODPs of 10 important ODSs. A substantial decrease in the lifetime estimates for HCFC-22, HCFC-141b and HCFC-142b and an increase in that of CH_3CCl_3 are observed when compared to the previous SF_6-age-based estimate of Laube et al. (2013). These changes do not cause large changes to the total atmospheric lifetimes of these gases; however, their main sink is the reaction with the OH radical in the troposphere. Our FRF and ODP calculations were further improved by the addition of a recent correction presented in Ostermöller et al. (2017). The interaction between these corrections is complex, but again it only results in substantial (but within ODP calculation uncertainties) changes for the three HCFCs (larger ODPs) and CH_3CCl_3 (smaller ODP) compared to Laube et al. (2013). Changes for all four compounds place our ODP estimates closer to the recommended ODPs in WMO (2014) than the values published in Laube et al. (2013).

The Supplement related to this article is available online at https://doi.org/10.5194/acp-18-3369-2018-supplement.

References

Andrews, A. E., Boering, K. A., Daube, B. C., Wofsy, S. C., Loewenstein, M., Jost, H., Podolske, J. R., Webster, C. R., Herman, R. L., Scott, D. C., Flesch, G. J., Moyer, E. J., Elkins, J. W., Dutton, G. S., Hurst, D. F., Moore, F. L., Ray, E. A., Romashkin, P. A., and Strahan, S. E.: Mean ages of stratospheric air derived from in situ observations of CO_2, CH_4, and N_2O, J. Geophys. Res.-Atmos., 106, 32295–32314, https://doi.org/10.1029/2001JD000465, 2001.

Arnold, T., Mühle, J., Salameh, P. K., Harth, C. M., Ivy, D. J., and Weiss, R. F.: Automated Measurement of Nitrogen Trifluoride in Ambient Air, Anal. Chem., 84, 4798–4804, https://doi.org/10.1021/ac300373e, 2012.

Barreto, H. and Howland, F.: Introductory Econometrics. Using Monte Carlo Simulation with Microsoft Excel, Cambridge University Press, New York, 2006.

Bönisch, H., Engel, A., Curtius, J., Birner, Th., and Hoor, P.: Quantifying transport into the lowermost stratosphere using simultaneous in-situ measurements of SF_6 and CO_2, Atmos. Chem. Phys., 9, 5905–5919, https://doi.org/10.5194/acp-9-5905-2009, 2009.

Bönisch, H., Engel, A., Birner, Th., Hoor, P., Tarasick, D. W., and Ray, E. A.: On the structural changes in the Brewer–Dobson circulation after 2000, Atmos. Chem. Phys., 11, 3937–3948, https://doi.org/10.5194/acp-11-3937-2011, 2011.

Brown, A. T., Volk, C. M., Schoeberl, M. R., Boone, C. D., and Bernath, P. F.: Stratospheric lifetimes of CFC-12, CCl_4, CH_4, CH_3Cl and N_2O from measurements made by the Atmospheric Chemistry Experiment-Fourier Transform Spec-

trometer (ACE-FTS), Atmos. Chem. Phys., 13, 6921–6950, https://doi.org/10.5194/acp-13-6921-2013, 2013.

Diallo, M., Legras, B., and Chédin, A.: Age of stratospheric air in the ERA-Interim, Atmos. Chem. Phys., 12, 12133–12154, https://doi.org/10.5194/acp-12-12133-2012, 2012.

Efron, B.: Bootstrap methods: another look at the jackknife, Ann. Stat., 7, 1–26, https://doi.org/10.1214/aos/1176348654, 1979.

Engel, A., Strunk, M., Müller, M., Haase, H.-P., Poss, C., Levin, I., and Schmidt, U.: Temporal development of total chlorine in the high-latitude stratosphere based on reference distributions of mean age derived from CO_2 and SF_6, J. Geophyis. Res., 107, ACH 1-1–ACH 1-11, https://doi.org/10.1029/2001JD000584, 2002.

Engel, A., Möbius, T., Haase, H.-P., Bönisch, H., Wetter, T., Schmidt, U., Levin, I., Reddmann, T., Oelhaf, H., Wetzel, G., Grunow, K., Huret, N., and Pirre, M.: Observation of mesospheric air inside the arctic stratospheric polar vortex in early 2003, Atmos. Chem. Phys., 6, 267–282, https://doi.org/10.5194/acp-6-267-2006, 2006.

Engel, A., Möbius, T., Bönisch, H., Schmidt, U., Heinz, R., Levin, I., Atlas, E., Aoki, S., Nakazawa, T., Sugawara, S., Moore, F., Hurst, D., Elkins, J., Schauffler, S., Andrews, A., and Boering, K.: Age of stratospheric air unchanged within uncertainties over the past 30 years, Nat. Geosci., 2, 28–31, https://doi.org/10.1038/ngeo388, 2009.

Engel, A., Bönisch, H., Ullrich, M., Sitals, R., Membrive, O., Danis, F., and Crevoisier, C.: Mean age of stratospheric air derived from AirCore observations, Atmos. Chem. Phys., 17, 6825–6838, https://doi.org/10.5194/acp-17-6825-2017, 2017.

Fraser, P., Oram, D., Reeves, C., Penkett, S., and McCulloch, A., Southern Hemisphere halon trends (1978–1998) and global halon emissions, J. Geophys. Res., 104, 15985–15999, https://doi.org/10.1029/1999JD900113, 1999.

Haenel, F. J., Stiller, G. P., von Clarmann, T., Funke, B., Eckert, E., Glatthor, N., Grabowski, U., Kellmann, S., Kiefer, M., Linden, A., and Reddmann, T.: Reassessment of MIPAS age of air trends and variability, Atmos. Chem. Phys., 15, 13161–13176, https://doi.org/10.5194/acp-15-13161-2015, 2015.

Hall, T. M. and Plumb, R. A.: Age as a diagnostic of stratospheric transport, J. Geophys. Res., 99, 1059–1070, https://doi.org/10.1029/93JD03192, 1994.

Harnisch, J., Borchers, R., Fabian, P., and Maiss, M.: CF_4 and the age of mesospheric and polar vortex air, Geophys. Res. Lett., 26, 295–298, https://doi.org/10.1029/1998GL900307, 1999.

Hoffmann, L., Hoppe, C. M., Müller, R., Dutton, G. S., Gille, J. C., Griessbach, S., Jones, A., Meyer, C. I., Spang, R., Volk, C. M., and Walker, K. A.: Stratospheric lifetime ratio of CFC-11 and CFC-12 from satellite and model climatologies, Atmos. Chem. Phys., 14, 12479–12497, https://doi.org/10.5194/acp-14-12479-2014, 2014.

Hooghiem, J., de Vries, M., Heikkinen, P., Kivi, R., and Chen, H.: A new lightweight active stratospheric air sampler. A presentation given at the 19th WMO/IAEA Meeting on Carbon Dioxide, Other Greenhouse Gases and Related Measurement Techniques (GGMT-2017) in Dübendorf, Switzerland 27–31 August 2017, abstract available at: https://www.empa.ch/web/ggmt2017/agenda, last access: 12 September 2017.

IPCC (Intergovernmental Panel on Climate Change): Hartmann, D. J., Klein Tank, A. M. G., Rusticucci, M., Alexander, L. V, Brön-nimann, S., Charabi, Y. A.-R., Dentener, F. J., Dlugokencky, E. J., Easterling, D. R., Kaplan, A., Soden, B. J., Thorne, P. W., Wild, M., and Zhai, P.: Observations: Atmosphere and Surface, chap. 2 in Climate Change 2013: The Physical Science Basis, Contribution of Working Group I to the Fifth Assessment Report of the Intergovernmental Panel on Climate Change (IPCC), edited by: Stocker, T. F., Qin, D., Plattner, G.-K., Tignor, M., Allen, S. K., Boschung, J., Nauels, A., Xia, Y., Bex, V., and Midgley, P. M., Cambridge University Press, Cambridge, UK and New York, USA, 159–254, 2013.

Kovács, T., Feng, W., Totterdill, A., Plane, J. M. C., Dhomse, S., Gómez-Martín, J. C., Stiller, G. P., Haenel, F. J., Smith, C., Forster, P. M., García, R. R., Marsh, D. R., and Chipperfield, M. P.: Determination of the atmospheric lifetime and global warming potential of sulfur hexafluoride using a three-dimensional model, Atmos. Chem. Phys., 17, 883–898, https://doi.org/10.5194/acp-17-883-2017, 2017.

Laube, J. C., Martinerie, P., Witrant, E., Blunier, T., Schwander, J., Brenninkmeijer, C. A. M., Schuck, T. J., Bolder, M., Röckmann, T., van der Veen, C., Bönisch, H., Engel, A., Mills, G. P., Newland, M. J., Oram, D. E., Reeves, C. E., and Sturges, W. T.: Accelerating growth of HFC-227ea (1,1,1,2,3,3,3-heptafluoropropane) in the atmosphere, Atmos. Chem. Phys., 10, 5903–5910, https://doi.org/10.5194/acp-10-5903-2010, 2010a.

Laube, J. C., Engel, A., Bönisch, H., Möbius, T., Sturges, W. T., Braß, M., and Röckmann, T.: Fractional release factors of long-lived halogenated organic compounds in the tropical stratosphere, Atmos. Chem. Phys., 10, 1093–1103, https://doi.org/10.5194/acp-10-1093-2010, 2010b.

Laube, J. C., Keil, A., Bönisch, H., Engel, A., Röckmann, T., Volk, C. M., and Sturges, W. T.: Observation-based assessment of stratospheric fractional release, lifetimes, and ozone depletion potentials of ten important source gases, Atmos. Chem. Phys., 13, 2779–2791, https://doi.org/10.5194/acp-13-2779-2013, 2013.

Laube, J. C., Mohd Hanif, N., Martinerie, P., Gallacher, E., Fraser, P. J., Langenfelds, R., Brenninkmeijer, C. A. M., Schwander, J., Witrant, E., Wang, J.-L., Ou-Yang, C.-F., Gooch, L. J., Reeves, C. E., Sturges, W. T., and Oram, D. E.: Tropospheric observations of CFC-114 and CFC-114a with a focus on long-term trends and emissions, Atmos. Chem. Phys., 16, 15347–15358, https://doi.org/10.5194/acp-16-15347-2016, 2016.

Li, F., Austin, J., and Wilson, J.: The strength of the Brewer-Dobson circulation in a changing climate: Coupled chemistry-climate model simulations, J. Climate, 21, 40–57, https://doi.org/10.1175/2007JCLI1663.1, 2008.

Mahieu, E., Chipperfield, M. P., Notholt, J., Reddmann, T., Anderson, J., Bernath, P. F., Blumenstock, T., Coffey, M. T., Dhomse, S. S., Feng, W., Franco, B., Froidevaux, L., Griffith, D. W. T., Hannigan, J. W., Hase, F., Hossaini, R., Jones, N. B., Morino, I., Murata, I., Nakajima, H., Palm, M., Paton-Walsh, C., Russell III, J. M., Schneider, M., Servais, C., Smale, D., and Walker, K. A.: Recent Northern Hemisphere stratospheric HCl increase due to atmospheric circulation changes, Nature, 515, 104–107, https://doi.org/10.1038/nature13857, 2014.

Miller, B. R., Weiss, R. F., Salameh, P. K., Tanhua, T., Greally, B. R., Mühle, J., and Simmonds, P. G.: Medusa: a sample preconcentration and GC-MS detector system for in situ measurements of atmospheric trace halocarbons, hydro-

carbons and sulfur compounds, Anal. Chem., 80, 1536–1545, https://doi.org/10.1029/2004GL022228, 2008.

Mühle, J., Ganesan, A. L., Miller, B. R., Salameh, P. K., Harth, C. M., Greally, B. R., Rigby, M., Porter, L. W., Steele, L. P., Trudinger, C. M., Krummel, P. B., O'Doherty, S., Fraser, P. J., Simmonds, P. G., Prinn, R. G., and Weiss, R. F.: Perfluorocarbons in the global atmosphere: tetrafluoromethane, hexafluoroethane, and octafluoropropane, Atmos. Chem. Phys., 10, 5145–5164, https://doi.org/10.5194/acp-10-5145-2010, 2010.

Newman, P. A., Nash, E. R., Kawa, S. R., Montzka, S. A., and Schauffler, S. M.: When will the Antarctic ozone hole recover?, Geophys. Res. Lett., 33, L12814, https://doi.org/10.1029/2005GL025232, 2006.

Newman, P. A., Daniel, J. S., Waugh, D. W., and Nash, E. R.: A new formulation of equivalent effective stratospheric chlorine (EESC), Atmos. Chem. Phys., 7, 4537–4552, https://doi.org/10.5194/acp-7-4537-2007, 2007.

Oberländer, S., Langematz, U., and Meul, S.: Unraveling impact factors for future changes in the Brewer-Dobson circulation, J. Geophys. Res.-Atmos., 118, 10296–10312, https://doi.org/10.1002/jgrd.50775, 2013.

O'Doherty, S., Rigby, M., Mühle, J., Ivy, D. J., Miller, B. R., Young, D., Simmonds, P. G., Reimann, S., Vollmer, M. K., Krummel, P. B., Fraser, P. J., Steele, L. P., Dunse, B., Salameh, P. K., Harth, C. M., Arnold, T., Weiss, R. F., Kim, J., Park, S., Li, S., Lunder, C., Hermansen, O., Schmidbauer, N., Zhou, L. X., Yao, B., Wang, R. H. J., Manning, A. J., and Prinn, R. G.: Global emissions of HFC-143a (CH_3CF_3) and HFC-32 (CH_2F_2) from in situ and air archive atmospheric observations, Atmos. Chem. Phys., 14, 9249–9258, https://doi.org/10.5194/acp-14-9249-2014, 2014.

Oram, D. E., Sturges, W. T., Penkett, S. A., McCulloch, A., and Fraser, P. J.: Growth of fluoroform (CHF_3, HFC-23) in the background atmosphere, Geophys. Res. Lett., 25, 35–38, https://doi.org/10.1029/97gl03483, 1998.

Ostermöller, J., Bönisch, H., Jöckel, P., and Engel, A.: A new time-independent formulation of fractional release, Atmos. Chem. Phys., 17, 3785–3797, https://doi.org/10.5194/acp-17-3785-2017, 2017.

Plumb, I., Vohralik, P. F., and Ryan, K. R.: Normalization of correlations for atmospheric species with chemical loss, J. Geophys. Res., 104, 11723–11732, https://doi.org/10.1029/1999JD900014, 1999.

Prinn, R. G., Weiss, R. F., Fraser, P. J., Simmonds, P. G., Cunnold, D. M., Alyea, F. N., O'Doherty, S., Salameh, P., Miller, B. R., Huang, J., Wang, R. H. J., Hartley, D. E., Harth, C., Steele, L. P., Sturrock, G., Midgley, P. M., and McCulloch, A.: A history of chemically and radiatively important gases in air deduced from ALE/GAGE/AGAGE, J. Geophys. Res., 105, 17751–17792, https://doi.org/10.1029/2000JD900141, 2000.

Ray, E. A., Moore, F., Rosenlof, K. H., Davis, S. M., Sweeney, C., Tans, P., Wang, T., Elkins, J. W., Bönisch, H., Engel, A., Sugawara, S., Nakazawa, T., and Aoki, S.: Improving stratospheric transport trend analysis based on SF_6 and CO_2 measurements, J. Geophys. Res.-Atmos., 119, 110–14128, https://doi.org/10.1002/2014JD021802, 2014.

Ray, E. A., Moore, F. L., Elkins, J. W., Rosenlof, K., Laube, J., Röckmann, T., Marsh, D. R., and Andrews, A. E.: Quantification of the SF_6 Lifetime Based on Mesospheric Loss Measured in the Stratospheric Polar Vortex, J. Geophys. Res.-Atmos., 122, 4626–4638, https://doi.org/10.1002/2016JD026198, 2017.

Rigby, M., Mühle, J., Miller, B. R., Prinn, R. G., Krummel, P. B., Steele, L. P., Fraser, P. J., Salameh, P. K., Harth, C. M., Weiss, R. F., Greally, B. R., O'Doherty, S., Simmonds, P. G., Vollmer, M. K., Reimann, S., Kim, J., Kim, K.-R., Wang, H. J., Olivier, J. G. J., Dlugokencky, E. J., Dutton, G. S., Hall, B. D., and Elkins, J. W.: History of atmospheric SF_6 from 1973 to 2008, Atmos. Chem. Phys., 10, 10305–10320, https://doi.org/10.5194/acp-10-10305-2010, 2010.

Singh, K. and Xie, M.: Bootstrap A Statistical Method, available at: http://stat.rutgers.edu/~mxie/RCPapers/bootstrap.pdf (last access: 20 March 2017), 2008.

SPARC – Chipperfield, M. P., Liang, Q., Abraham, N. L., Bekki, S., Braesicke, P., Dhomse, S., Di Genova, G., Fleming, E. L., Hardiman, S., Iachetti, D., Jackman, C. H., Kinnison, D. E., Marchand, M., Pitari, G., Rozanov, E., Stenke, A., and Tummon, F.: chap. 5: Model Estimates of Lifetimes, in SPARC Report on the Lifetimes of Stratospheric Ozone-Depleting Substances, Their Replacements, and Related Species, SPARC Report No. 6, WCRP-15/2013, available at: www.sparc-climate.org/publications/sparc-reports/ (last access: 8 February 2018), edited by: Newman, P. A., Reimann, S., and Strahan, S. E., https://doi.org/10.1029/1999JD901128, 2013.

Stiller, G. P., von Clarmann, T., Höpfner, M., Glatthor, N., Grabowski, U., Kellmann, S., Kleinert, A., Linden, A., Milz, M., Reddmann, T., Steck, T., Fischer, H., Funke, B., López-Puertas, M., and Engel, A.: Global distribution of mean age of stratospheric air from MIPAS $SF6$ measurements, Atmos. Chem. Phys., 8, 677–695, https://doi.org/10.5194/acp-8-677-2008, 2008.

Stiller, G. P., Fierli, F., Ploeger, F., Cagnazzo, C., Funke, B., Haenel, F. J., Reddmann, T., Riese, M., and von Clarmann, T.: Shift of subtropical transport barriers explains observed hemispheric asymmetry of decadal trends of age of air, Atmos. Chem. Phys., 17, 11177–11192, https://doi.org/10.5194/acp-17-11177-2017, 2017.

Strunk, M., Engel, A., Schmidt, U., Volk, C. M., Wetter, T., Levin, I., and Glatzel-Mattheier, H.: CO_2 and SF_6 as stratospheric age tracers: consistency and the effect of mesospheric SF_6-loss, Geophys. Res. Lett., 27, 341–344, https://doi.org/10.1029/1999GL011044, 2000.

Trudinger, C. M., Fraser, P. J., Etheridge, D. M., Sturges, W. T., Vollmer, M. K., Rigby, M., Martinerie, P., Mühle, J., Worton, D. R., Krummel, P. B., Steele, L. P., Miller, B. R., Laube, J., Mani, F. S., Rayner, P. J., Harth, C. M., Witrant, E., Blunier, T., Schwander, J., O'Doherty, S., and Battle, M.: Atmospheric abundance and global emissions of perfluorocarbons CF_4, C_2F_6 and C_3F_8 since 1800 inferred from ice core, firn, air archive and in situ measurements, Atmos. Chem. Phys., 16, 11733–11754, https://doi.org/10.5194/acp-16-11733-2016, 2016.

Volk, C. M., Elkins, J. W., Fahey, D. W., Dutton, G. S., Gilligan, J. M., Loewenstein, M., Podolske, J. R., Chan, K. R., and Gunson, M. R.: Evaluation of source gas lifetimes from stratospheric observations, J. Geophys. Res., 102, 25543–25564, https://doi.org/10.1029/97JD02215, 1997.

von Hobe, M., Bekki, S., Borrmann, S., Cairo, F., D'Amato, F., Di Donfrancesco, G., Dörnbrack, A., Ebersoldt, A., Ebert, M., Emde, C., Engel, I., Ern, M., Frey, W., Genco, S., Griessbach,

S., Grooß, J.-U., Gulde, T., Günther, G., Hösen, E., Hoffmann, L., Homonnai, V., Hoyle, C. R., Isaksen, I. S. A., Jackson, D. R., Jánosi, I. M., Jones, R. L., Kandler, K., Kalicinsky, C., Keil, A., Khaykin, S. M., Khosrawi, F., Kivi, R., Kuttippurath, J., Laube, J. C., Lefèvre, F., Lehmann, R., Ludmann, S., Luo, B. P., Marchand, M., Meyer, J., Mitev, V., Molleker, S., Müller, R., Oelhaf, H., Olschewski, F., Orsolini, Y., Peter, T., Pfeilsticker, K., Piesch, C., Pitts, M. C., Poole, L. R., Pope, F. D., Ravegnani, F., Rex, M., Riese, M., Röckmann, T., Rognerud, B., Roiger, A., Rolf, C., Santee, M. L., Scheibe, M., Schiller, C., Schlager, H., Siciliani de Cumis, M., Sitnikov, N., Søvde, O. A., Spang, R., Spelten, N., Stordal, F., Suminska-Ebersoldt, O., Ulanovski, A., Ungermann, J., Viciani, S., Volk, C. M., vom Scheidt, M., von der Gathen, P., Walker, K., Wegner, T., Weigel, R., Weinbruch, S., Wetzel, G., Wienhold, F. G., Wohltmann, I., Woiwode, W., Young, I. A. K., Yushkov, V., Zobrist, B., and Stroh, F.: Reconciliation of essential process parameters for an enhanced predictability of Arctic stratospheric ozone loss and its climate interactions (RECONCILE): activities and results, Atmos. Chem. Phys., 13, 9233–9268, https://doi.org/10.5194/acp-13-9233-2013, 2013.

WMO (World Meteorological Organization): Scientific Assessment of Ozone Depletion: 2014, World Meteorological Organization, Global Ozone Research and Monitoring Project – Report No. 55, Geneva, Switzerland, 2014.